

A Broadband and Cost-Effective Fermi Antenna for W-band Imaging System

Dong Sik Woo, Jin Hyun Park, Young Gon Kim, Young Ki Cho and #Kang Wook Kim
College of IT Engineering, Kyungpook National University
1370 Sankyuck-Dong Bukgu Daegu KOREA, kang_kim@ee.knu.ac.kr

Abstract

A broadband and high gain Fermi antenna by utilizing a broadband microstrip (MS)-to-coplanar stripline (CPS) balun is presented on low dielectric permittivity substrate. This antenna exhibits the ultra-wideband performance for the frequency range of over 110 GHz with the high antenna gain, low sidelobe levels and narrow beamwidth. This antenna can be alternatives to cost-effective millimeter-wave imaging systems and phased-arrays.

Keywords : Fermi Antenna Tapered Slot Antenna Coplaner stripline Balun W-band

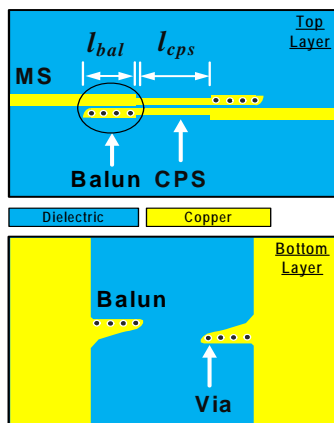
1. Introduction

Electromagnetic waves in the millimeter-wave band have attractive characteristics. One of their features is the wider usable frequency band compared with waves in the microwave band or lower bands. Tapered slot antenna (TSA) is the most popular printed end-fire antenna, which are often used for microwave/millimeter-wave imaging, sensors and phased-arrays. This antenna produces many advantages such as broad bandwidth, high gain, narrow beamwidth and symmetrical radiation patterns [1]. TSA called a “Fermi antenna” with Fermi-Dirac distribution is already reported by S. Sugawara and H. Sato *et al.* [2-4]. Fermi antenna have many design parameters such as feeding balun structure, taper profile, length and the width of aperture, and shape of corrugations [3]. In order to feed balanced radiators, various types of balun have been reported in many literatures. However, conventional planar baluns such as MS-to-slotline, MS-to-CPS, coplanar waveguide (CPW)-to-slotline and double Y balun impose limits on frequency bandwidth of the antenna [5-8]. In this paper, broadband and low-cost W-band Fermi antenna has been obtained by utilizing the ultra-wideband MS-to-CPS balun [9] on low dielectric permittivity substrate. The antenna dimensions and its radiation properties are demonstrated.

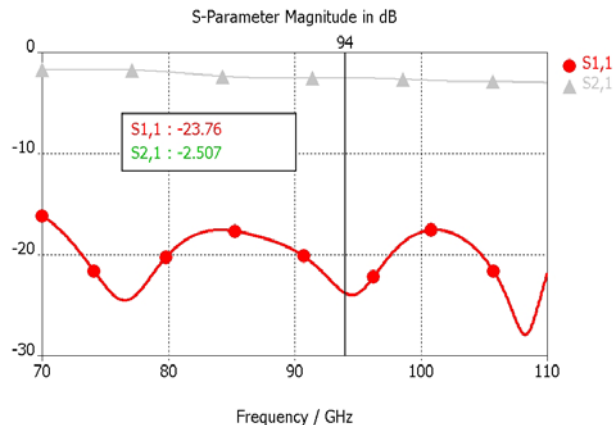
2. Antenna Design

2.1 Microstrip-to-coplanar stripline balun design

The design of the Fermi antenna is simplified in two steps: the design of the balun and the design of the slotline-fed Fermi antenna with the CPS impedance of the blaun. Firstly, an ultra-wideband MS-to-CPS balun is designed by following the outline in [9] as shown in Fig. 1.



(a) Top and bottom layer of the balun



(b) Simulated return loss

Figure 1: Microstrip-to-CPS balun

The broadband characteristic of the balun usually covers the whole frequency bandwidth of the Fermi antenna. The field matching and impedance matching techniques are used by controlling the taper shape of the ground plane. In this paper, the characteristic impedance of the CPS is chosen about 139Ω with 5 mil gap between CPS strips and 20 mil strip width using a 10-mil Duroid 5880[®] ($\epsilon_r = 2.2$) substrate. With the CPS length (l_{cps}) of 180 mil and the transition length (l_{bal}) of 130 mil, the simulated insertion loss per transition is less than 1.5 dB from 70 to over 110 GHz as shown in Fig. 1. The antenna is simulated with CST Microwave[™], and cross-checked with ANSOFT HFSS[™] V10.

2.2 Fermi Antenna Design

The Fermi antenna with the Fermi-Dirac tapering function with corrugated edges [2-4] is designed at W-band. The slotline-fed Fermi antenna is optimized with the characteristics impedance of the CPS. Figure 2 shows the fabricated antenna and its design parameters. The low permittivity substrate Duroid 5880[®] ($\epsilon_r = 2.2$) with 10-mil thickness is used. The Antenna's dimensions are (unit: mil): $L=502(4\lambda_0)$, $w_i=64$, $w_o=88(0.7\lambda_0)$, $w_g=5$, $d=24$, $w_c=w_d=5$, $l_c=19$, $l_{bal}=130$, $l_{tran}=90$.

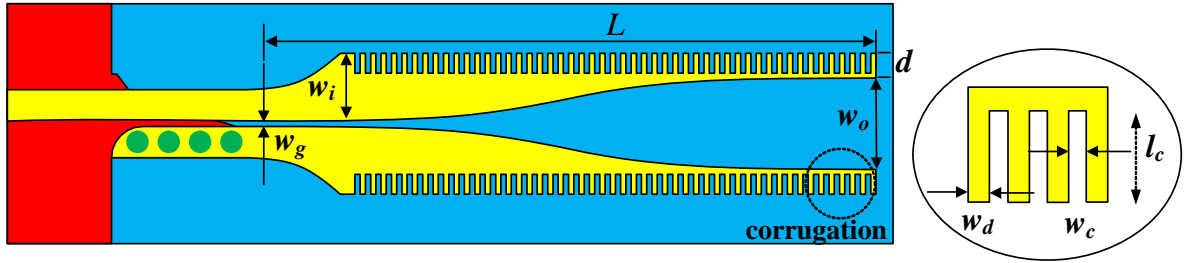


Figure 2: The geometry of the proposed Fermi antenna

The Fermi-Dirac tapering function $f(x)$ and its parameters are determined to optimize the radiation patterns using following equations:

$$f(x) = \frac{a}{1 + e^{-b(x-c)}} \quad b = \frac{2.4}{\lambda_0} \quad c = 2\lambda_0 \quad (1)$$

, where λ_0 is free space wavelength at the center frequency, a is the asymptotic value of the taper for x approaches infinity, and x is the variable of the taper length. The length of the antenna (L) is chosen as $4\lambda_0$ at 94 GHz. The opening width w_o can be varied to obtain the desired radiation patterns. The corrugation on upper and lower sides of the Fermi antenna is commonly used to suppress the surface-mode waves excited on the dielectric substrate and sidelobe level, to obtain higher gain, to improve the VSWR, to widen the effective aperture size of antenna. The dimensions of the corrugation (w_d, w_c, l_c) are chosen by [3] ($w_c = L/100$, $l_c = 0.15\lambda_0$). The antenna size is 21.6×5.6 mm. Finally, by connecting this MS-to-CPS balun to radiators, the overall Fermi antenna design is completed.

3. Simulation Results and Applications

The simulated return losses demonstrating ultra-wideband performance better than 10 dB from 60 to over 110 GHz as shown in Fig. 3. The overall bandwidth of the antenna is almost the same as that of the slotline-fed radiators; i.e., the CPS feed and the balun provide wide bandwidth and impedance matching so that they do not change the bandwidth of the original Fermi antenna. The mutual coupling is also investigated by the simulated transmission coefficient S21 for array environment. The horizontal center-to-center spacing between antennas is 230 mil ($1.8\lambda_0$). In most cases, the simulated mutual coupling is below -40 dB for whole W-band. For understanding the propagation characteristics of the antenna, the surface current distributions (J_s) are presented at frequencies 70, 94 and 110 GHz, respectively. The propagation behaviors are figured out along the open end. And the transverse wave is also reduced by corrugations as shown in Fig. 4.

Figure 5 shows the simulated E- and H-plane radiation patterns at 70, 94 and 110 GHz, respectively. A low sidelobe levels and symmetrical radiation patterns are achieved with low cross-polarization levels. The performance of the Fermi antenna is summarized in Table 1. The antenna gain maintains from 13 to 14 dBi with low sidelobe levels of less than -10 dB from 70 to 110 GHz. The 3-dB beamwidth ranges from 28° to 34° for E-plane and 36° to 39° for H-plane with good radiation efficiency (84~89%).

From these results, the validity of this antenna is verified for broadband and cost-effective imaging systems at W-band. Therefore, they can be used mm-wave camera under low-visibility condition, sensors can detect concealed weapons or explosive materials and wide-band millimeter-wave holographic surveillance system. In addition, this antenna is also useful for finding landmines, for detecting cracks in exterior walls, and for screening people for skin cancer.

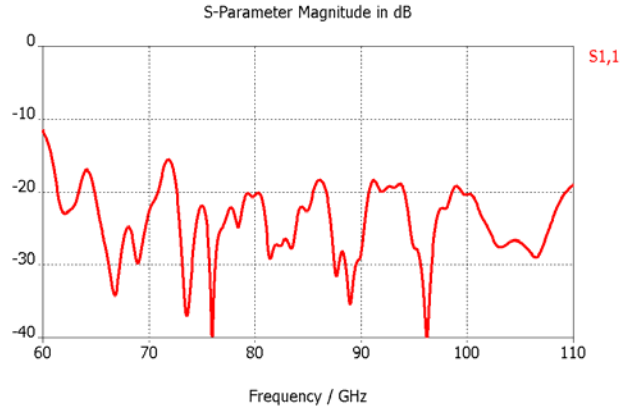


Figure 3: Simulated return loss

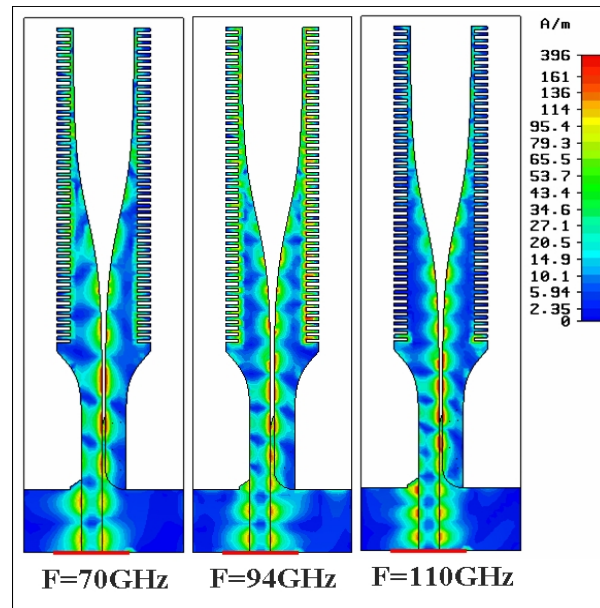


Figure 4: Surface current distributions at 70, 94 and 110 GHz

Table 1: The performance summary of the antenna

	Gain [dBi]	3-dB BW [degree]		SLL [dB]		Radiation Efficiency (%)
		E-plane	H-plane	E-plane	H-plane	
70 GHz	13.6	33.6	38.6	-17.6	-14.7	89
94 GHz	13.7	28.2	36.5	-15.5	-11	84
100 GHz	14.1	27.6	37	-17.4	-10.7	85
110 GHz	13.9	28.7	38.4	-15.2	-8.6	86

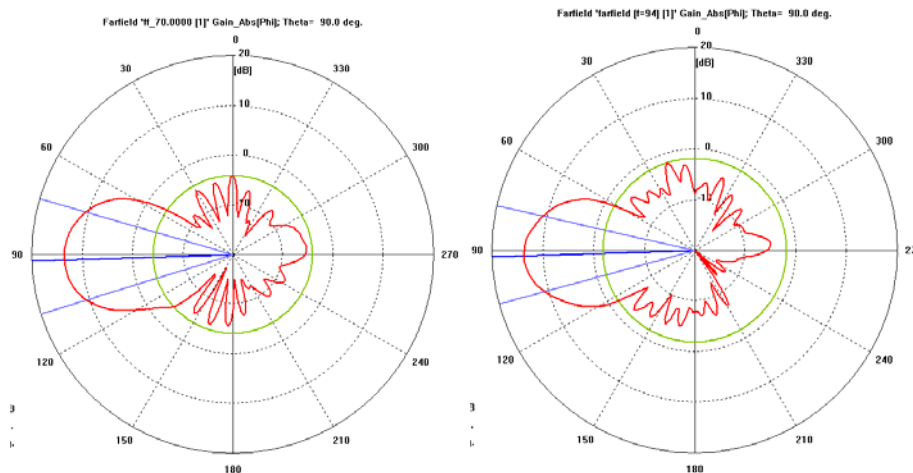


Figure 5: Simulated E-plane radiation patterns at 70/94 GHz

4. Conclusion

A simplified design guideline for a broadband and high directivity W-band Fermi antenna using MS-to-CPS balun is introduced. This Fermi antenna consists of a MS-to-CPS balun section and Fermi-Dirac tapered slot antenna with corrugation. Simulation results demonstrate symmetrical radiation patterns, narrow beamwidth, and low sidelobe levels for whole frequency ranges from 70 to 110 GHz and above. The proposed antenna can be applied to various broadband and cost-effective planar millimeter-wave imaging systems.

References

- [1] K. F. Lee and W. Chen, *Advances in Microstrip and Printed Antennas*, John Wiley & Sons, New York, NY, 1997.
- [2] H. Sato, K. Sawaya, N. Arai, Y. Wagatsuma and K. Mizuno, "FDTD Analysis of Fermi tapered slot antenna with corrugation structure," *China-Japan Joint Meeting on Microwaves (CJMW2002)*, pp.137-140, 2002
- [3] H. Sato, K. Sawaya, Y. Wagatsuma, and K. Mizuno, "Broadband FDTD design of fermi antenna for passive millimeter wave imaging," *IEEE Int. Symp. MAPE.*, pp.123-126, 2005.
- [4] K. Sawaya, H. Sato, Y. Wagatsuma, and K. Mizuno, "Broadband Fermi antenna and its application to mm-wave imaging," *Antennas and Propagation Conference(EuCAP 2007)*, pp.1-6, 2007.
- [5] R. N. Simons, N. I. Dib, R. Q. Lee, and L. P. B. Katehi, "Integrated unipolar transition for linearly tapered slot antenna," *IEEE Trans. Antennas Propagat.*, vol.43, no.9, pp.998-1002, 1995.
- [6] W. H. Tu and K. Chang, "Wide-band microstrip-to-coplanar stripline/slotline transitions," *IEEE Trans. Microwave Theory Tech.*, vol. 54, no. 3, pp. 1084–1089, 2006.
- [7] L. Yang, N. Ito, C. W. Domier, N. C. Luhmann, and A. Mase, "18–40-GHz Beam-shaping/steering phased antenna array system using Fermi antenna," *IEEE Trans. Microwave Theory Tech.*, vol. 56, no. 4, pp.767-773, 2008.
- [8] K. Ma and T. Itoh, "Analysis and applications of a new CPW-slotline transition," *IEEE Trans. Microwave Theory Tech.*, vol. 47, no. 4, pp. 426–432, 1999.
- [9] Y. G. Kim, D. S. Woo, K. W. Kim, and Y. K. Cho, "A new ultra-wideband microstrip-to-CPS transition," *IEEE MTT-S Int. Microw. Symp. Dig.*, pp.1563-1566, 2007.

Acknowledgments

This research was supported by the MKE(The Ministry of Knowledge Economy), Korea, under the CITRC(Convergence Information Technology Research Center) support program (NIPA-2011-C6150-1102-0011) supervised by the NIPA(National IT Industry Promotion Agency)